HTR2008
September 28-October 1, 2008, Washington, DC USA

HTR2008-58276

PERFORMANCE COMPARISON OF VHTR PLANTS WITH DIRECT AND INDIRECT ENERGY CONVERSION CYCLES

Mohamed S. El-Genk and Jean-Michel Tournier
Institute for Space and Nuclear Power Studies and Chemical and Nuclear Engineering Department
University of New Mexico, Albuquerque, NM 87131, USA

ABSTRACT

This paper compared the performance of very high temperature reactor (VHTR) plants with direct and indirect closed Brayton Cycles (CBCs) and investigated the effect of the molecular weight of the CBC working fluid on the number of stages in and the size of the single shaft turbo-machines. The CBC working fluids considered are helium (4 g/mole) and He-Xe and He-N_2 binary mixtures (15 g/mole). Also investigated are the effects of using LPC and HPC with inter-cooling, cooling the reactor pressure vessel with He bled off at the exit of the compressor, and changing the reactor exit temperature from 700°C to 950°C on the plant thermal efficiency, CBC pressure ratio and the number of stages in and size of the turbo-machines. Analyses are performed for reactor thermal power of 600 MW, shaft rotation speed of 3000 rpm, and IHX temperature pinch of 50 °C.

1. INTRODUCTION

Helium-cooled, very high temperature reactor (VHTR) concepts with direct and indirect Closed Brayton Cycles (CBCs) for energy conversion are being developed in the USA, Europe, Russia, Japan and South Africa [1-4]. Reactor exit temperatures of 850 °C - 950 °C make it possible to operate at plant thermal efficiency > 40% and provide process heat for the co-generation of hydrogen using thermo-chemical processes [1-4] and a host of industrial applications, but pose challenges to the materials selection for the Reactor Pressure Vessel (RPV), heat exchangers, and the fuel performance, to mention a few. In order to use steel alloys, bleed cooling of RPV would be necessary to keep the vessel wall temperature below 371°C (644 K), which is only an option with direct CBC (Fig. 1) [5, 6]. In another arrangement being considered, the returning gas to the reactor cools the RPV wall to or below 490°C (763 K) before entering the reactor core. This relatively high vessel wall temperature favors using Mo-Cr alloys, requiring further development and testing and hence, a long lead time for deployment and eventual use.

Recent studies have shown that while helium has the best transport and thermal properties of all noble gases, its low molecular weight (4 g/mole) significantly increases the size and number of stages of the CBC turbo-machines [7,8]. Mixing helium with xenon to a binary mixture molecular weight of 15 g/mole increases the forced convection heat transfer coefficient by ~ 7% and significantly reduces the aerodynamic loading of the compressor and turbine blades. The latter translates into few stages in and smaller size of the turbo-machines [7]. Similar results have been reported for He-N_2 binary mixture with the same molecular weight [8].

While nitrogen is relatively inexpensive and more abundant than xenon, there are concerns with potential nitriding and embrittlement of the structure. In addition, these gas species decrease the excess reactivity of the reactor due to neutron capture and raise concerns regarding radioactive contamination of the CBC loop components with irradiation products, particularly ^{125}Xe ($T_{1/2}$=16.9h) and ^{134}Cs ($T_{1/2}$ = 2.06y), which emit high energy gammas, and ^{14}C ($T_{1/2}$=5715y) and ^{3}H ($T_{1/2}$=12.32y), which emit beta particles [9]. Therefore, the use of the binary mixtures of He-Xe and He-N_2 should be limited to indirect CBCs (Fig. 1b).

VHTR plants being considered use both direct and indirect CBC for energy conversion (Figs. 1a and 1b). With direct coupling, the reactor coolant is also the CBC working fluid, lowering the reactor exit temperature for the same turbine inlet temperature, and simplifying the plant layout. However, it complicates maintenance and permits the transport of radioactivity to the CBC turbo-machines. These concerns are alleviated in plants with indirect CBC, but at the expense of increasing the reactor temperature and/or decreasing the plant thermal efficiency (Fig. 1b). Indirect coupling of the CBC to the reactor allows using helium for cooling the reactor and the higher molecular binary mixtures as CBC working fluids, reducing the size and number of stages of the turbo-machines. In addition to minimizing the impact of changing the electrical load demand on the reactor operation, indirect CBC coupling provides flexibility in maintenance and operation and for supplying process heat to

the hydrogen generation facility, but decrease the plant thermal efficiency.

Using low pressure compressor (LPC) and high pressure compressor (HPC) with inter-cooling in direct and indirect CBCs decreases the compression work and the coolant bleed fraction for cooling the electrical generator, turbine disks and shaft bearings (Figs. 1a and 1b). With direct CBC, bleeding off helium at the exit of the compressor to cool the RPV is used in the Japanese GTHTR300 plant design [5, 6] (Fig. 1a). In this plant, bleeding off only 0.2% of the flow was enough [5] to keep the RPV wall temperature at or below 371 ^{o}C (644 K). *Such RPV cooling, however, is not practically possible with indirect CBCs.* Thus, with indirect CBCs, the temperature of the helium entering the reactor is kept constant at or below 490 ^{o}C (763 K) [10], as in the GT-MHR [4] and the NGNP [1, 3] plants (Fig. 1b).

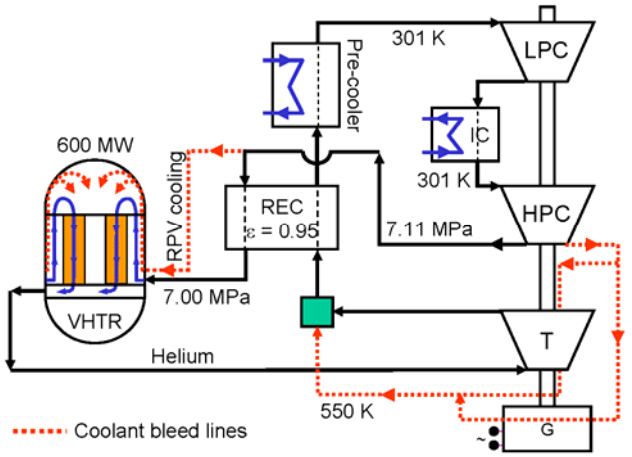

(a) VHTR plant with direct CBC

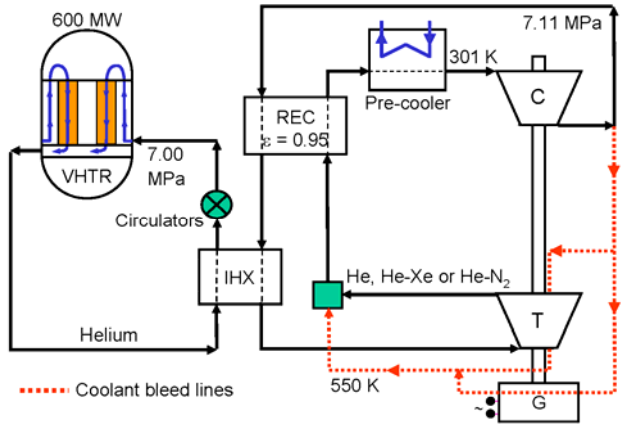

(b) VHTR plant with indirect CBC

Fig. 1. Direct and Indirect Closed Brayton Cycles

To determine the impact of using direct or indirect CBC with different working fluids on the thermal efficiency, size and number of stages of the CBC turbo-machines, detailed models of the compressor and the turbine are developed and validated. The developed design models of the multi-stage, axial flow, single shaft turbo-machines, only briefly summarised in this paper, are used to calculate the impacts of changing the hardware, CBC working fluid, and shaft rotation speed on the polytropic efficiencies, and the size in and the number of stages of the compressor and turbine [8]. The developed models have been validated for the GTHTR300 compressor and turbine [11, 12] in helium, direct CBC (Fig. 1a). Results, including the number of stages, the polytropic efficiencies and pressure ratios, showed excellent agreement with reported values [8].

This paper also investigates the effect of the molecular weight of the CBC working fluid on the performance of VHTR plant with indirect CBC. The fluids considered are helium in direct CBC plants and helium and binary mixtures of He-Xe and He-N_2 (15 g/mole) in indirect CBC plants. Also investigated are the effects of using LPC and HPC with inter-cooling, cooling the RPV in the plants with direct CBC using helium bled off at the exit of the compressor (Fig. 1a), and changing the reactor exit temperature from 700 ^{o}C to 950 ^{o}C on the plant thermal efficiency, cycle pressure ratio and polytropic efficiency, and number of stages in and size of the turbo-machines. Analyses are performed for shaft rotation speed of 3000 rpm, reactor thermal power of 600 MW and a 50 ^{o}C temperature pinch in the IHX (Fig. 1b).

2. MODELS DESCRIPTION

The present turbo-machines models are based on a mean-line analysis of vortex free flow along the blades [13-17]. The compressor and turbine are designed for constant axial flow velocity, V_x in the stages and constant mean-line blade radius, r_m. In all stages, the mean flow coefficient, φ_m, is kept constant, assuming uniform loading coefficient, λ_m and reaction, $\Re_m$. The gas flow enters the first stages of the turbine and compressor axially, $V_{in} = V_x$, and exits the last stages also axially, $V_{ex} = V_x$.

Typical velocity triangles at the leading and trailing edges of the turbine and compressor rotor blades cascade are shown in Figs. 2a and 2b in orthogonal coordinates (x, θ). The coordinate x coincides with the axis of the turbo-machines, and θ is the angular coordinate. Subscripts 1 and 2 refer to the cascade inlet and exit stations. The absolute velocity in the stationary coordinate system, V, becomes W in the rotating coordinate system. The tangential velocity of the rotating blades, $U = U_\theta$, and α and ϕ are the absolute and relative velocity angles. For the compressor blades, the gas turning angle is much smaller than for the turbine, limiting the separation of the boundary layer due to a positive pressure gradient.

In addition to the velocity triangles, other input to the present turbo-machines models include the inlet flow ($\dot{N}$, P_{in} and T_{in}), the shaft total mechanical work, $\dot{W}$, the number of rotor stages, and the shaft rotational speed, ω. The blades aspect ratio for the compressor stators H/C = 1.7, and 1.4 for all other blades. The maximum thickness ratio for the turbine

blades, t_{max}/C = 0.2, and 0.1 for the compressor blades (Fig. 3). The trailing edge thickness ratio for all turbine cascades, except the EGVs, t_{TE} / S = 0.02 [16, 17]; while for all compressor cascades, t_{TE}/C = 0.00046 (same as for the symmetric NACA 65A010 compressor airfoils [14]). The blades tip clearance, τ = 1 mm, and number of tip seals are specified in the input to models, when the blades are shrouded [5, 6]. For the compressor blades and turbine EGVs, the assumed relative position of the maximum camber, Z/C = 0.5. The thermodynamic and transport properties of the working fluids in the turbo-machines models are calculated using reported semi-empirical relationships developed and validated successfully against a large experimental database for temperature from 300 – 1400 K and pressure up to 20 MPa [7, 18, 19].

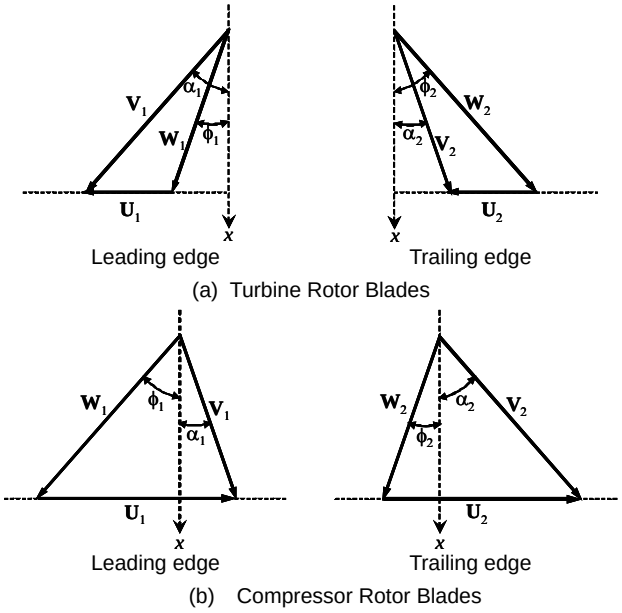

Fig. 2. Velocity Triangles for Turbine and Compressor

2.1 Compressor Model

The present compressor model accounts for the profile and secondary pressure losses, and the end wall and tip clearance losses. The profile loss coefficient is calculated using the approach by Koch and Smith [20]. The secondary flow loss coefficient is calculated using the correlation proposed by Howell [21], and the end wall losses are calculated using the approach of Aungier [14]. The tip clearance losses are calculated using the model of Yaras and Sjolander [22] for the turbine blades, after substituting $\cos(\phi_2)$ for $\cos(\phi_1)$, since the compressor blade losses are calculated based on the inlet flow conditions.

The values of (Z/C), the maximum camber (b/C), and the blade angles measured from the chord line (χ_1 and χ_2) uniquely define the parabolic-arc camberline profile [14] of the compressor blades (Figs. 3b and 4). The blades camber (or turning) angle: $\theta = \chi_1 + \chi_2 = \beta_1 - \beta_2$. The leading edge (LE) and trailing edge (TE) angles of the blades, β_1 and β_2, are calculated from the determined optimum incidence and deviation angles. The compressor model assumes a solidity, σ = 1.10 for the IGVs, and computes the optimum solidity for the other cascades using a correlation developed based on the optimum values of σ that minimize the sum of the profile and the secondary flow loss coefficients.

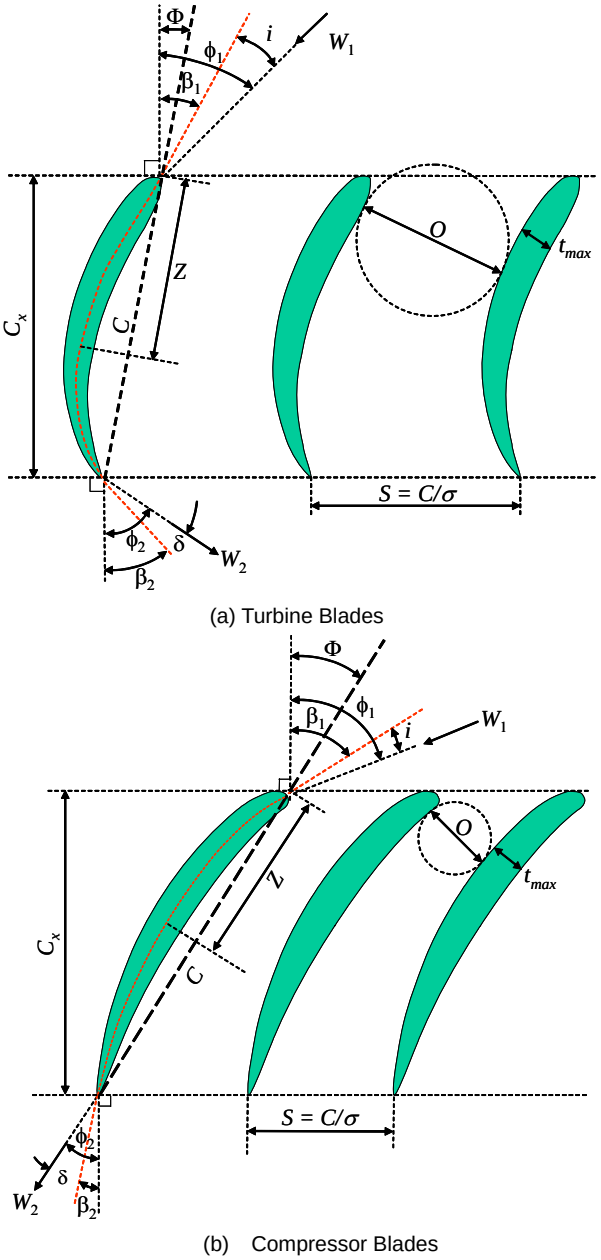

Fig. 3. Turbine and Compressor Blade Cascades

2.2 Turbine Model

The parabolic-arc camberline profile (Figs. 3a and 4) is also used in the present turbine model, but with caution, to predict the blades cascades geometry. The turning angle and the maximum thickness of the turbine blades are larger that those of the compressor blades, and $\beta_1 < \beta_2$. The blades

camber (or turning) angle in the turbine is given by: $\theta = \chi_1 + \chi_2 = \beta_1 + \beta_2$. The optimum solidity for the turbine blades cascade is calculated using the correlation by Aungier [15], based on matching the Ainley-Mathieson [17] minimum profile loss coefficient. The turbine blades are designed for a zero incidence angle and the deviation angle at the trailing edge is calculated using a recent correlation by Zhu and Sjolander [23].

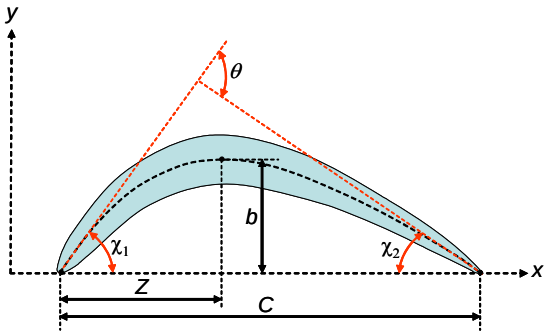

Fig. 4. Blade Profile with Parabolic-Arc Camberline

Because the turning angle of turbine blades is larger than in compressor, their parameters are very sensitive to the value of maximum camber position, (Z/C) that may not be known accurately. Therefore, the present turbine model uses the values recommended by Kacker and Okapuu [16] for predicting the stagger angle of typical turbine blades cascades, Φ, as a function of β_1 and β_2. This stagger angle is used to determine the blades angles with respect to the chord line (Fig. 4). The maximum camber location [Z/C, b/C] is determined from simultaneously solving equations describing the blade shape. The losses in the turbine are calculated using recommended correlation from various sources [24 – 26].

3. PLANT ANALYSES

The performed plant analyses assume recuperator effectiveness of 0.95, constant compressor inlet temperature of 301 K, reactor thermal power of 600 MW and reactor inlet pressure of 7.0 MPa (Figs. 1a and 1b). The pressure losses in the cold and hot legs of the recuperator and in the pre- and inter-coolers are assumed 1.5% and 1.9%, and 1.5% of the inlet pressure (Figs. 1a and 1b). The assumed shaft mechanical efficiency is 99% and the generator efficiency is 98.7%, for shaft rotation speed of 3000 rpm (50 Hz). The analyses also assume fixed flow channels dimensions in the VHTR core. Thus, the pressure losses in the reactor vary with the molar flow rate of the coolant, $\dot{N}$, raised to the power 1.8, and the molecular weight and dynamic viscosity raised to the power of 0.8 and 0.2, [7]:

$$(\Delta P/P) \propto \left(T/P^2\right) \dot{N}^{1.8} \left(\mu^{0.2} M^{0.8}\right).$$

For the helium plants with direct or indirect CBCs (Figs. 1a and 1b), the bled off flow at the exit of the compressor is used to cool the turbine casing and disks, shaft bearings and the electrical generator, and in the direct CBC also cools the RPV wall to $\leq$ 371 ^{o}C (644 K) (Fig. 1a). With RPV bleed cooling, the inlet temperature to the reactor core increases freely as the reactor exit temperature increases. For the plants with He, and He-Xe and He-N_2 (15 g/mole) indirect CBCs, the working fluid bled off at the exit of the compressor is only used to cool the turbo-machines and the electrical generator (Fig. 1b), and the He inlet temperature to the VHTR is kept constant at 490^{o}C (763 K).

The bled off flow is calculated assuming a temperature of 550 K at the inlet of the mixing chamber (Figs. 1a and 1b). This temperature is dictated by the electrical insulation of the generator. The bled off flow for cooling the turbo-machines and electrical generator varies from 1% to 13%. In the plants with indirect CBCs, analyses assume a 50 ^{o}C temperature pinch in IHX (Fig. 1b). The pressure losses in the IHX primary leg are taken equal to 1.7% of the inlet pressure. The electrical power to circulate the primary loop helium (Fig. 1b), calculated assuming a circulator isentropic efficiency of 87%, varies from 10 to 35 MWe, depending on operating conditions. As a result, when heat looses are neglected the thermal power transferred to the CBC loop through the IHX would vary between 610 and 635 MW.

4. RESULTS AND DISCUSSION

The present performance analyses of the VHTR plants with direct and indirect CBCs, with and without inter-cooling, are performed for reactor exit temperatures of 973 – 1223 K (Figs. 1a and 1b). For the helium plants with direct CBCs, the analyses are performed with and without RPV bleed cooling. For the plants with He, He-Xe and He-N_2 indirect CBCs, the analyses are performed for a constant reactor inlet temperature of 490 ^{o}C (763 K).

4.1 Direct He-CBC Plants with RPV Cooling

The results showing the effects of implementing RPV bleed cooling on the performance of the VHTR plants with direct He-CBC are shown in Figs. 5a and 5b, with and without inter-cooling. Without inter-cooling, there is only one compressor, while with inter-cooling, the LPC and HPC operate at the same inlet temperature of 301 K and the same compression ratio (Figs. 1a and 1b). When cooling the RPV with helium bled off at the HPC exit, the plant operates near its peak thermal efficiency. The relatively low cycle pressure ratio (2.25 – 2.3) increases very little as the reactor exit temperature increases (Figs. 5a and 5b).

The nominal operation points of the VHTR plants with inter-cooling are indicated by the blue circular solid symbols in Fig. 5b. The corresponding plant thermal efficiency increases steadily with increasing the reactor exit temperature, but remains very close to the peak efficiency (Fig. 5b). It increases steadily from 41.8% to 51.5% as the reactor exit temperature increases from 973 K to 1223 K. The reactor

inlet temperature also increases from 721 K to 886 K as its exit temperature increases from 973 to 1223 K. Without inter-cooling, the reactor inlet temperature is slightly higher than with inter-cooling, increasing from 755 K to 932 K as the reactor exit temperature increases from 973 K to 1223 K (Fig. 5a). The non-intercooled direct He-CBC delivers lower plant thermal efficiency than the inter-cooled cycle (Fig. 5b). The plant thermal efficiency increases steadily from 38.4% to 47.6% as the reactor exit temperature increases from 973 K to 1123 K (Fig. 5a).

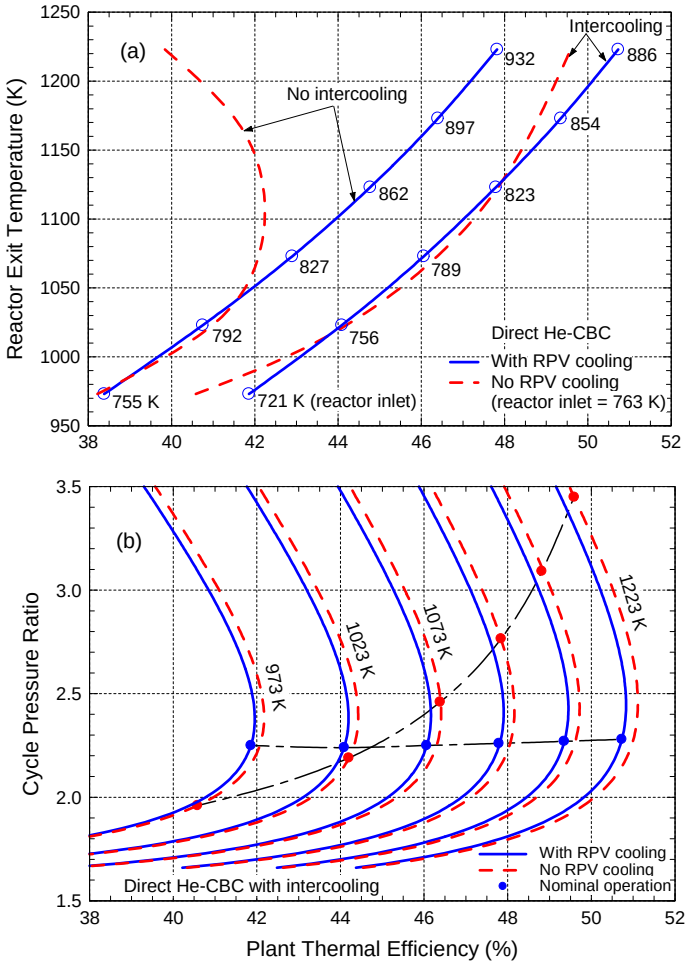

Fig. 5. Effect of RPV Cooling on Performance of Direct He-CBC VHTR Plants

By contrast, without bleed cooling, the RPV is cooled with circulated helium, keeping the inlet temperature to the reactor constant at 490 °C, and the cycle pressure ratio increases, but the plant thermal efficiency decreases as the reactor exit temperature increases (Figs. 5a and 5b). Without RPV bleed cooling, when the reactor exit temperature is >1023 K, the thermal efficiency of the plant without inter-cooling decreases steadily and the cycle pressure ratio increases with increasing the reactor exit temperature. The plant thermal efficiency is much lower and the cycle pressure ratio is much higher than the plant with inter-cooling (Figs. 5a and 5b). For reactor exit temperatures <1023 K, both the plant thermal efficiency and the pressure ratio of the direct He-CBC without inter-cooling are lower than those with inter-cooling.

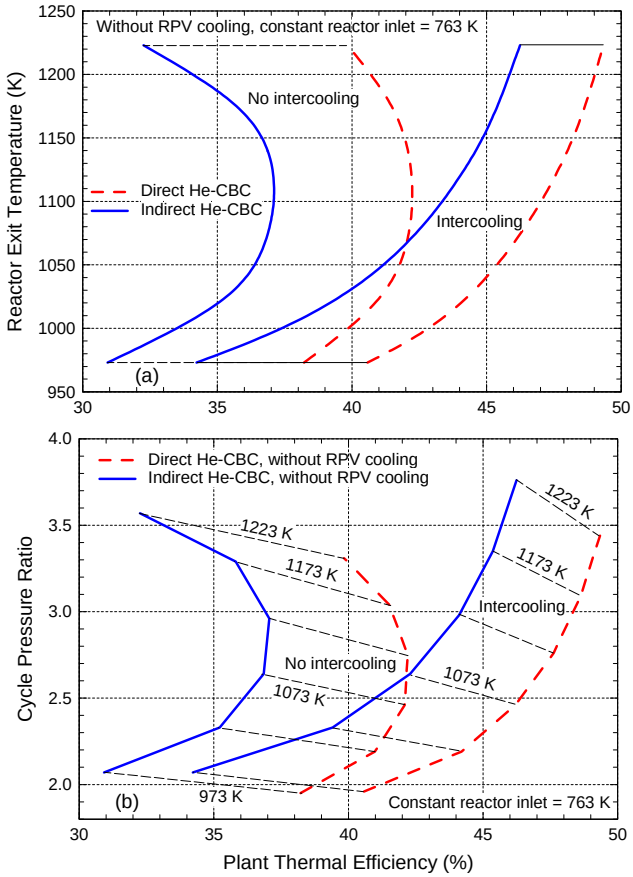

Fig. 6. Direct and Indirect He-CBC VHTR Plants without RPV Cooling

The differences in the thermal efficiency and the cycle pressure ratio of the plants without RPV bleed cooling and inter-cooling are significantly lower and higher than those of the plants with RPV bleed cooling, but without inter-cooling. The results in Figs. 5a and 5b clearly indicate that for the best performance of the VHTR plants with direct He-CBCs, using RPV cooling and LPC and HPC with inter-cooling are recommended. The latter, however, increases the combined number of stages and the size of the compressors, as will be shown later in Figure 8 and 9. The pressure ratio of the LPC and HPC is much lower than that of the single non-intercooled compressor, and the temperature at the exit of the compressors is lower, resulting in lower bleed fraction for cooling the generator and shaft bearings (Fig. 1a).

4.2 Direct and Indirect He-CBC without RPV Cooling

Figures 6a and 6b compare the performance of the VHTR plants with direct and indirect He-CBC, with and without inter-cooling, but without bleed cooling of the RPV. These plants operate at a constant reactor inlet temperature of 490 °C

(763 K). For the same reactor exit temperature, the plants with inter-cooling operate at slightly higher cycle pressure ratios, but significantly higher thermal efficiencies. Using inter-cooling steadily increases the plant thermal efficiency as the reactor exit temperature increases. Without inter-cooling, the plant efficiency increases with increased reactor exit temperature up to ~ 1123 K, then decreases with further increase in the exit temperature (Figs. 6a and 6b). The difference in the performance of the plants with indirect and direct He-CBCs is essentially due to the 50 K pinch in the IHX (Fig. 1b). Thus, for the same reactor exit temperature, the turbine in the indirect He-CBC operates cooler than in the direct cycle, resulting in 5.5 – 7.5 percentage points decrease in the thermal efficiency of the plant with no inter-cooling, and 3 - 6 percentage points drop in the efficiency of the plant with inter-cooling.

4.3 Plants Performance with Indirect CBCs

This section compares the performance of VHTR plants with indirect CBCs, with and without inter-cooling, and without RPV bleed cooling (Figs. 7a and 7b). The results for He-Xe and He-N_2 working fluids (15 g/mole) are compared with those of helium, at the same reactor exit temperature. With He-N_2 and He-Xe binary mixture working fluids, the pressure losses in the CBC loop increase by a factor 2.7, compared to those in the He CBC [7], when operating at same temperature, pressure and molar flow rate. Thus, when using He-N_2 or He-Xe (15 g/mole), the present analyses assume the diameters of the flow channels in the indirect CBC loop increase by 23% in order to maintain the same relative pressure losses as with helium [7]. The turbines for the higher molecular weight working fluids (He-N_2 and He-Xe, 15 g/mole) are designed using a higher mean-radius flow coefficient of 0.60 (compared to 0.433 for He), which corresponds to near optimum polytropic efficiency [13,15].

Figures 7a and 7b show the effects of the CBC working fluid on the performance of the VHTR plants with indirect CBCs. For the same reactor exit temperature, the plants with indirect He and He-Xe CBCs operate at the same cycle pressure ratio (Fig. 7b). This is because He-Xe behaves essentially as a pure noble gas with a specific heat ratio of ~ 1.67. By contrast, the plant with indirect He-N_2 CBC operates at a higher cycle pressure ratio (Fig. 7a), because He-N_2 of the same molecular weight of 15 g/mole has a lower specific heat ratio (~ 1.45) [7,8,19]. The plants with inter-cooling operate at slightly higher cycle pressure ratios than the non-intercooled plants, because of higher pressure losses in the former (Fig. 7b).

The plants with non-intercooled He-N_2, indirect CBC deliver higher performance than the ones with non-intercooled He-CBC, at reactor exit temperatures < 1090 K (Fig. 7a). This is because the He-N_2 turbine and compressor have higher polytropic efficiencies (93.2% and 90.9%) than their He counterparts. At higher reactor exit temperatures, however, the plant with non-intercooled indirect He-N_2 CBC has lower thermal efficiency than that with indirect He-CBC. This is because the former operates at a higher cycle pressure ratio, which translates into higher compressor exit temperature and higher bleed flow for cooling the shaft bearings and electrical generator (Fig. 1b).

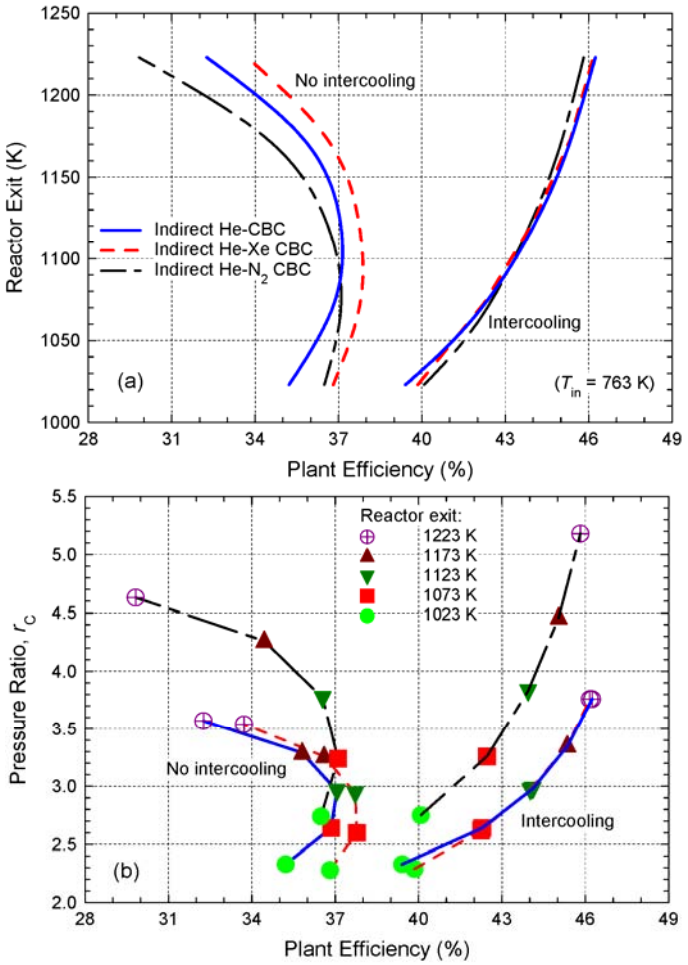

Fig. 7. Indirect CBC VHTR Plants without RPV Cooling

The thermal efficiency of the VHTR plant with indirect He-Xe CBC but without inter-cooling is 1 - 1.6 percentage points higher than the plant with indirect He-CBC (Fig. 7a). The two CBCs operate at the same pressure ratio, but the higher-molecular weight turbine and compressor are more efficient, having polytropic efficiencies of 93.3% and 90.8%. By contrast, the helium turbine and compressor have polytropic efficiencies of 92.3% and 90.5%, which are nearly independent of the VHTR exit temperature, using the design rules of this work.

The VHTR plants with inter-cooled, indirect CBCs operate at higher thermal efficiencies than the plants without inter-cooling (Fig. 7a). The CBC working fluid has very little effect on the thermal efficiency of the plants employing indirect CBCs with inter-cooling. The turbine has the same polytropic efficiency as that in the non-intercooled CBC, but

the LPC and HPC are slightly less efficient than the single compressor in the CBC without inter-cooling. The polytropic efficiencies of the He, He-Xe and He-N_2 LPCs are 90.3%, 90.3% and 90.4%, and those of the HPCs are 90.1%, 90.1% and 90.4%, respectively.

4.3 Effect of Working Fluid on Turbo-machines Size

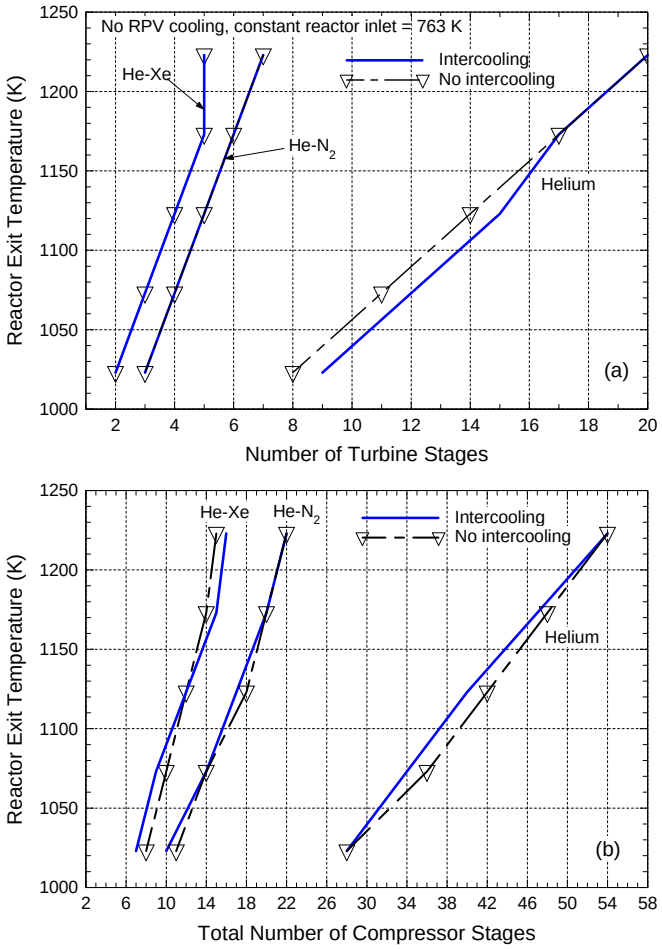

Fig. 8. Number of Stages in Turbo-machinery with He, He-Xe and He-N_2 Indirect-CBCs

For the plants employing direct He-CBCs with RPV bleed cooling, increasing the reactor exit temperature increases both its inlet temperature and the number of stages in the turbine and compressor. With inter-cooling in the CBC, the combined number of stages of the helium LPC and HPC are higher than of the single compressor in the CBC without inter-cooling. Also, the number of stages in the helium turbine for the CBC with inter-cooling is higher than without. For the direct He-CBC without inter-cooling, when operating at a reactor exit temperature of 1173 K the turbine has 8 stages and the compressor has 25 stages By contrast, for the direct He-CBC with inter-cooling, the turbine has 11 stages. The LPC has 13 stages and the HPC has 18 stages, for a total of 31 stages.

As shown in Figures 8a and 8b, the number of stages in the He-Xe and He-N_2 turbo-machinery for the indirect CBCs are considerably smaller than in the He-CBC, when operating at the same reactor exit temperature. The size and the number of stages in the turbine and the compressor, however, increase as the reactor exit temperature increases (Figs. 8a and 8b). At a reactor exit temperature of 900°C (1173 K), the He-Xe turbine has only 5 stages and the He-N_2 turbine has 6 stages, compared to the 17 stages in the helium turbine (Figs. 8a and 9).

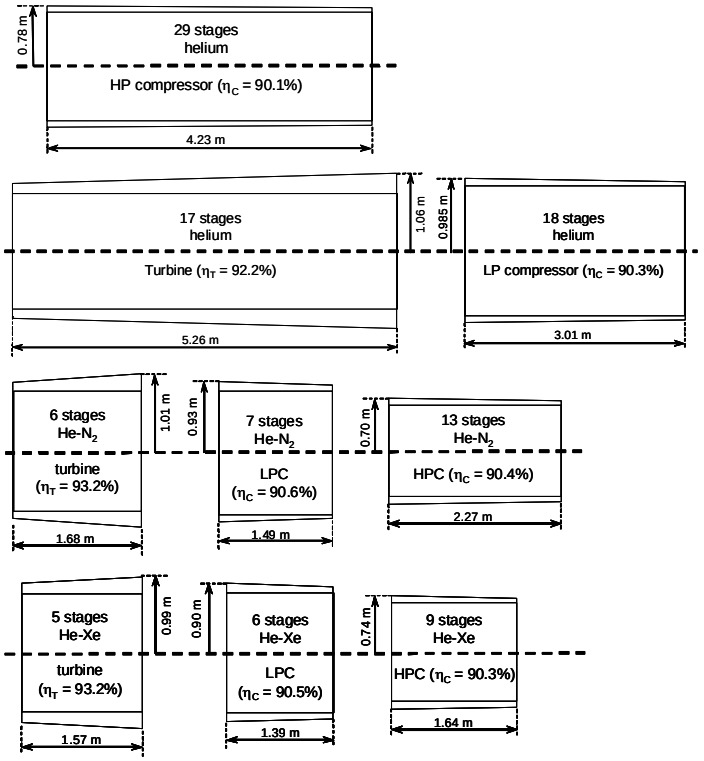

Fig. 9. Comparison of the Size and Dimensions of Single-Shaft Turbo-machines with Inter-cooling

Similarly, the plants with He-Xe and He-N_2 indirect CBCs require 15 and 20 compression stages, compared to 47 stages for the He plant (Figs. 8b and 9). As a result, the rotor shafts of the He-N_2 and He-Xe turbo-machines are a factor 2 and 3 shorter that for helium turbo-machines (Fig. 9). In addition to the reduced capital cost of the turbo-machines, shorter shafts have better dynamic stability and longer operation life and are more reliable. Also, for these shafts the lighter rotor's bearings are easier to design.

6. SUMMARY AND CONCLUSIONS

Design models of multi-stage, axial flow turbo-machines for CBCs are developed and the effect of the molecular weight of the working fluid on the performance, number of stages in and the size of the compressor and turbine are investigated. The CBC working fluids considered are helium in plants with direct and indirect CBCs and the binary

mixtures of He-Xe and He-N_2 with a molecular weight of 15 g/mole for the plants with in indirect CBCs.

The analyses investigated the effects on the plant thermal efficiency, cycle pressure ratio and the number of stages in and the size of the turbo-machines of the following: (a) using LPC and HPC with inter-cooling in direct and indirect CBCs; (b) cooling the VHTR pressure vessel with He bled off at the exit of the compressor versus cooling the RPV wall with returning helium with a constant inlet temperature of 490 ^{o}C in the plants with direct He-CBCs; and (c) changing the reactor exit temperature from 700^{o}C to 950^{o}C.

Cooling the RPV with bled off helium is considered only an option for the plants with direct helium CBCs (Fig. 1a). It is impractical for the VHTR plants with indirect CBCs with He and binary mixtures of He-Xe and He-N_2. The plant performance analyses are performed for shaft rotation speed of 3000 rpm, reactor thermal power of 600 MW and temperature pinch of 50 ^{o}C in the IHX for the plants with indirect CBCs (Fig. 1b). Based on the obtained performance results of the VHTR plant with different CBC arrangements and different working fluids, the following conclusions are reached:

(a) In VHTR plants with direct He-CBCs, when the reactor exit temperature > 1023 K – 1073 K (750 - 800^{o}C), using bleed cooling of RPV and LPC and HPC with inter-cooling are highly recommended. The thermal efficiency of the plant is highest, and the cycle compression ratio is relatively low and increases very little as the reactor exit temperature increases. Therefore, these choices are strongly recommended for VHTR plants with direct He-CBC, when operating at reactor exit temperatures > 1023 K – 1073 K.

(b) At reactor exit temperatures < 1073 K, without bleed cooling and maintaining the reactor inlet temperature constant at 490 ^{o}C, using LPC and HPC with inter-cooling lowers the cycle pressure ratio and slightly lowers the plant thermal efficiency than in (a) above. Thus, this plant layout may be used when the reactor exit temperature is 1023 K – 1073 K.

(c) Using LPC and HPC with inter-cooling in both direct and indirect CBCs steadily increase the cycle pressure ratio, the plant thermal efficiency, and the reactor inlet temperature as the reactor exit temperature increases. However, for the same cycle pressure ratio, inter-cooling significantly increases the thermal efficiency of the plant.

(d) With indirect CBCs and LPC and HPC with inter-cooling, the plant thermal efficiency is higher than without inter-cooling, and almost independent of the molecular weight of the working fluid, but increases steadily with increased reactor exit temperature.

(e) Inter-cooling in the plants with direct He-CBCs and RPV bleed cooling decreases the reactor inlet temperature but increases the number of the compressor and turbine stages. The number of the stages also increases as the reactor exit temperature increases.

(f) In the helium plants employing CBCs without inter-cooling, the number of stages of the turbo-machines is fewer than for the CBCs with inter-cooling, but the reactor inlet temperature is higher.

(g) In the plants with indirect CBCs and working fluids of He-Xe and He-N_2 (15 g/mole), the number of stages of the compressor and the turbine are significantly fewer and the length of the rotating shaft is much shorter than for helium turbo-machines. Such reduction in the size and mass of the turbo-machines for the He-Xe and He-N_2 working fluids translate into considerable cost saving, higher operation reliability and lower maintenance.

NOMENCLATURE

b	Maximum camber of blade (m)
C	Actual chord length of blade (m), Compressor
C_x	Axial chord length of blade (m), $C_x = C \times \cos\Phi$
EGVs	Exit guide vanes
H	Height of blades (m)
HPC	High pressure compressor
IGVs	Inlet guide vanes
LPC	Low pressure compressor
M	Molecular weight (kg/mole)
$\dot{N}$	Molar flow rate (mole/s)
P	Pressure (Pa)
r	Radius (m)
$\Re$	Stage reaction
S	Pitch or distance between blades in cascade (m)
t_{max}	Maximum blade thickness (m)
t_{TE}	Thickness of blades trailing edge (m)
T	Temperature (K), Turbine
U	Rotor tangential velocity (m / s), $U = r\omega$
V_x	Gas meridional velocity component (m / s)
V_θ	Gas tangential velocity component (m / s)
$\vec{W}$	Gas relative velocity vector (m/s), $\vec{W} = \vec{V} - \vec{U}$
Z	Position of maximum camber (m)

Greek

α	Angle between gas absolute velocity vector and meridional plane (^{o})
β	Blade angle relative to meridional plane (degrees)
ΔP	Total pressure loss (Pa)
ε	Recuperator effectiveness
θ	Blade camber (or turning) angle (^{o})
λ	Stage loading (work) coefficient, $\lambda = \Delta\hat{h}_{st} / U^2$
μ	Coolant dynamic viscosity (kg / m.s)
ρ	Density (kg / m^3)
σ	Blade cascade solidity, $\sigma = C / S$
τ	Blades clearance gap (m)
φ	Stage flow coefficient, $\varphi = V_X / U$

ϕ Angle between gas relative velocity vector and meridional plane (^{o})
Φ Blades stagger angle measured from axial direction (^{o})
χ Blade angle measured from the chord line (^{o})
ω Shaft angular speed (radians / s)

Subscript / Superscript

θ Tangential or "whirl" component
IHX Intermediate heat exchanger
LE Leading edge of blades
m Median location of annular flow passage
TE Trailing edge of blades
x, z Axial component
1 Inlet or leading edge of rotor blades cascade
2 Exit or trailing edge of rotor blades cascade

ACKNOWLEDGMENTS

This research is sponsored by the University of New Mexico's Institute of Space and Nuclear Power Studies.

REFERENCES

1. *Next Generation Nuclear Plant – Pre-Conceptual Design Report*, INEEL/EXT-07-12967 Rev. 1, Idaho National Engineering and Environmental Laboratory (November 2007).
2. C. H. Oh, R. Barner, C. Davis and S. Sherman, "Evaluation of Working Fluids in an Indirect Combined Cycle in a Very High Temperature Gas-Cooled Reactor," *Nuclear Technology*, **156**, 1 – 10 (2006).
3. G. A. Johnson, "Power Conversion System Evaluation for the Next Generation Nuclear Plant (NGNP)," *Proc. International Congress on Advances in Nuclear Power Plants (ICAPP 08)*, American Nuclear Society, Paper # 8253, Anaheim, CA, USA, 8-12 June 2008.
4. H. C. No, J. H. Kim and H. M. Kim, "A Review of Helium Gas Turbine Technology for High-Temperature Gas-Cooled Reactors," *Nuclear Engineering and Technology*, **39** (1), 21 – 30 (2007).
5. X. Yan, K. Kunitomi, T. Nakata and S. Shiozawa, "Design and Development of GTHTR300," *Proc. 1st International Topical Meeting on HTR Technology (HTR2002)*, held in Petten, Netherlands, April 22 – 24, 2002, International Atomic Energy Agency, Vienna, Austria, 2002.
6. X. Yan, T. Takizuka, S. Takada, K. Kunitomi, I. Minatsuki and Y. Mizokami, "Cost and Performance Design Approach for GTHTR300 Power Conversion system," *J. Nucl. Eng. and Design*, **226**, 351 – 373 (2003).
7. M. S. El-Genk, M. S. and J.-M. Tournier, "Noble Gas Binary Mixtures for Gas-Cooled Reactor Power Plants," *J. Nucl. Eng. and Design* **238**, 1353 – 1372 (2008).
8. J.-M. Tournier and M. S. El-Genk, "Alternative Working Fluids to Reduce Size of Turbomachinery for VHTR Plants," *Proc. International Congress on Advances in Nuclear Power Plants (ICAPP 08)*, American Nuclear Society, Paper # 8072, Anaheim, CA, USA, 8-12 June 2008.
9. T. M. Schriener and M. S. El-Genk, "Neutronic Performance of High Molecular Weight Coolants for a Prismatic VHTR," *Proc. International Congress on Advances in Nuclear Power Plants (ICAPP 08)*, American Nuclear Society, Paper # 8104, Anaheim, CA, USA, 8-12 June 2008.
10. A. V. Vasyaev, V. F. Golovko, I. V. Dimitrieva, N. G. Kodochigov, N. G. Kuzavkov and V. M. Rulev, "Substantiation of the Parameters and Layout Solutions for an Energy Conversion Unit with a Gas-Turbine Cycle in a Nuclear Power Plant with HTGR," *Atomic Energy*, **98** (1), 21 – 31 (2005).
11. K. Kunitomi, S. Katanishi, S. Takada. X. Yan, and N. Tsuji, "Reactor Core Design of Gas Turbine High Temperature Reactor 300," *J. Nucl. Eng. and Design*, **230**, 349 – 366 (2004).
12. T. Takizuka, S. Takada, X. Yan, S. Kosugiyama, S. Katanishi, and K. Kunitomi, "R&D on the Power Conversion System for Gas Turbine High Temperature Reactors," *J. Nucl. Eng. and Design* **233**, 329 – 346 (2004).
13. L. Fielding, T*urbine Design – The Effect on Axial Flow Turbine Performance of Parameter Variation*, ASME Press, New York, NY, pp. 130 – 132 (2000).
14. R. H. Aungier, *Axial-Flow Compressor – A Strategy for Aerodynamic Design and Analysis*, ASME Press, New York, NY, Chapter 6, pp. 118 – 152 (2003).
15. R. H. Aungier, *Turbine Aerodynamics - Axial-Flow and Radial-Inflow Turbine Design and Analysis*, ASME Press, New York, NY, pp. 69 – 79 (2006).
16. S. C. Kacker and U. Okapuu, "A Mean Line Prediction Method for Axial Flow Turbine Efficiency," *Journal of Engineering for Power*, **104**, 111 – 119 (1982).
17. D. G. Ainley and G. C. R. Mathieson, *A Method of Performance Estimation for Axial-Flow Turbines*, British Aeronautical Research Council, Reports and Memoranda No. 2974, December 1951.
18. J.-M. Tournier and M. S. El-Genk, "Properties of Noble Gases and Binary Mixtures for Closed Brayton Cycle Applications," *J. Energy Conversion and Management, **49** (3)*, 469 – 492 (2008).
19. J.-M. Tournier and M. S. El-Genk, "Properties of Helium, Nitrogen, and He-N_2 Binary Gas Mixtures," *Journal of Thermophysics and Heat Transfer, **22** (3)* (2008).
20. C. C. Koch and L. H. Smith, Jr., "Loss Sources and Magnitudes in Axial-Flow Compressors," *Journal of Engineering for Power*, **A98**, 411 – 424 (1976).
21. Howell, A. R., *Fluid Dynamics of Axial Compressors*, Lectures on the Development of the British Gas Turbine

Jet Unit, War Emergency Proc. No. **12**, Institution of Mechanical Engineers (Great Britain), pp. 441 – 452 (1947).
22. M. I. Yaras and S. A. Sjolander, "Prediction of Tip-Leakage Losses in Axial Turbines," *Journal of Turbo-Machinery*, **114**, 204 – 210 (1992).
23. J. Zhu and S. A. Sjolander, "Improved Profile Loss and Deviation Correlations for Axial-Turbine Blade Rows," in *Proc. GT2005 ASME Turbo Expo 2005: Power for Land, Sea and Air*, Reno-Tahoe, Nevada, USA, American Society of Mechanical Engineers, New York, NY, Paper No. GT2005-69077, pp. 783-792, June 6-9, 2005.
24. M. W. Benner, S. A. Sjolander and S. H. Moustapha, "An Empirical Prediction Method for Secondary Losses in Turbines – Part I: A New Loss Breakdown Scheme and Penetration Depth Correlation," *Journal of Turbo-Machinery*, **128**, 273 – 280 (2006).
25. M. W. Benner, S. A. Sjolander and S. H. Moustapha, "An Empirical Prediction Method for Secondary Losses in Turbines – Part II: A New Secondary Loss Correlation," *Journal of Turbo-Machinery*, **128**, 281 – 291 (2006).
26. T. Matsunuma, "Effects of Reynolds Number and Freestream Turbulence on Turbine Tip Clearance Flow," *Journal of Turbo-Machinery*, **128**, 166 – 177 (2006).

